Strain Relief during Growth: CaF_2 on Si(111)

R. M. Tromp, F. K. LeGoues, and M. C. Reuter
IBM Research Division, T. J. Watson Research Center, P.O. Box 218, Yorktown Heights, New York 10598
(Received 7 July 1994)

The growth of thin CaF_2 films on Si(111) was studied with *in situ* low energy electron microscopy and transmission electron microscopy. As the strained epitaxial film passes through the critical thickness, initial dislocations form in triplets ("trigons"). These serve as sources for full edge dislocations which subsequently form a dense network. This unusual dislocation structure provides a natural explanation for a recently proposed "two-dimensional structure modulation" of the Si(111)/CaF_2 interface.

PACS numbers: 61.16.–d, 61.72.Ff, 68.35.Ja

Van der Merwe discussed the equilibrium structure of a thin epitaxial film several decades ago [1]. Above the critical thickness the energy cost of a misfit dislocation is offset by the relief of misfit strain. The exact thickness at which misfit dislocations become favorable depends on the degree of misfit between substrate and overlayer, the elastic properties, and the type of dislocation. In many systems dislocations may be readily available, i.e., there are many low energy sources, such as bulk crystal defects, impurities, etc. However, this is not always the case, and the question of how and where which dislocations first form is of critical importance. Unfortunately, dislocation nucleation is not sufficiently well understood to make general predictions. In fact, few experimental studies are available in which the relaxation mechanism has been followed in real time and real space, from the first stages of interface formation to beyond the critical thickness. One early study, on the growth of Pd on Au(111) by Cherns and Stowell [2], shows similarities with our results on the growth of CaF_2 on Si(111), as we will discuss later. Here, we detect not only the presence of dislocations, but we see where they first form, how they move and interact (both with other dislocations and with interface steps), and how they gradually densify into a network. In the end we find dissociated, full edge dislocations with the Burgers vector in the interface plane, not previously identified in this system [3,4]. Regions between partial dislocations contain interfacial stacking faults, explaining the recent "two-dimensional structure modulation" proposed on the basis of x-ray scattering studies [5]. However, the relaxation process does not begin with edge dislocations. Instead, a triplet of $1/2\langle 110\rangle$ dislocations is nucleated on the inclined {001} planes, in a triangular geometry (termed a "trigon" by Cherns and Stowell). The full edge dislocations emanate from the corners of these trigons and grow slowly by the climb of a threading dislocation that terminates at the surface. The trigons first form near the center of the largest interface terraces where strain is highest, and never near the interface steps which have partial dislocation character [4].

The complexity and richness of this process underlines the importance of understanding the dislocation nucleation process, and the necessity of real time, *in situ* studies. We have used low energy electron microscopy (LEEM) to follow the growth of CaF_2, recording the process on videotape. Low energy electrons (typically less than 10 eV in our LEEM experiments) provide a gentle probe for studying CaF_2 growth without radiation damage. Recently, we have shown how LEEM can be used to image interface structure in slightly out-of-focus bright field imaging conditions [6]. By somewhat varying electron energy and focusing conditions *either* the Si/CaF_2 interface *or* the CaF_2 surface can be observed, which we used to study the relation between dislocation nucleation and surface morphology. All LEEM images presented are stills taken from videotape. The LEEM instrument has been described elsewhere [7]. In addition, we have used transmission electron microscopy (TEM) to determine the dislocation character in detail, using a Philips 420 electron microscope at 120 keV electron energy.

CaF_2 was grown in Si(111) at 770 °C. At this temperature a well-ordered interface is formed, with Ca atoms bonding to the (1×1) Si substrate [8]. The CaF_2 film is twinned relative to the substrate (*B*-type epitaxy). Steps on the Si substrate result in interface steps between Si and CaF_2. Because of the *B*-type stacking these interface steps have partial dislocation character and locally relieve misfit strain [9]. As growth is started, the (7×7) reconstruction is removed, and at one layer coverage a CaF_1 interfacial layer is formed with Ca adsorbed on a Si T_4 site [8,10]. (Ca may be adsorbed on two different sites: T_4 over a second-layer atom, or H_3 over a fourth-layer atom. The presence of Ca on H_3 sites [5,11] will be discussed later.) The second layer forms by nucleation and growth of 2D islands on the terraces, but these do not cross the interface steps. To cross the step requires the formation of a dislocation core, which is energetically not yet favorable. At this stage the interface steps resemble the "coreless" dislocations proposed some years ago in the very similar Si(111)/$CoSi_2$ system [12]. The third layer overgrows the interface step edge. Because of isolated

 0031-9007/95/74(14)/2706(4)$06.00

nucleation and growth in 2D on isolated terraces, the surface is rather rough at this point. However, once the interface steps are overgrown step-flow growth takes over, and the surface becomes smooth. Nothing interesting happens until the critical thickness (~30 Å) is reached.

Figure 1 shows a sequence in which the nucleation of dislocations can be followed in detail. In Fig. 1(a) we observe interface steps (diagonal lines), as well as the first trigons near the center of the widest interface terraces (arrows). With increasing thickness [Figs. 1(b) and 1(c)] arms grow out of these triangles, extending across the surface, interacting with each other, and finally forming a dislocation network. Since the interface steps have partial dislocation character and relieve misfit strain, the dislocations (trigons) first appear where strain is highest, near the center of the widest terraces. While LEEM is sensitive to the dislocation strain field, it cannot determine the Burgers vector of the dislocation. This was done with TEM. Figure 2(a) is a bright field image showing a trigon with dislocations extending from the corners, as well as two interface steps. The arms are seen to consist of two parallel dislocations, not resolved with LEEM. Figures 2(b)–2(d) show a $\mathbf{g} \cdot \mathbf{b}$ analysis. A dislocation is extinguished in the image if its Burgers vector is perpendicular to the diffraction vector used to form the image (i.e., $\mathbf{g} \cdot \mathbf{b} = 0$). Using the three $\langle 2\bar{2}0 \rangle$ diffraction vectors each of the dislocation lines in Fig. 2(a) can be extinguished. We conclude that these are either $1/6\langle 11\bar{2} \rangle$ or $1/2\langle 110 \rangle$ type dislocations. (The primary glide system in CaF_2 consists of $1/2\langle 110 \rangle$ dislocations gliding on {001} planes.) Images obtained with the bulk-forbidden $1/3\langle 422 \rangle$ reflection [see arrow in the inset in Fig. 2(a)] reveal the presence of an interface stacking fault between the parallel dislocations in the arms, showing that they are partial dislocations. The central triangular area of the trigon is not faulted. By following the morphology of steps on the CaF_2 surface

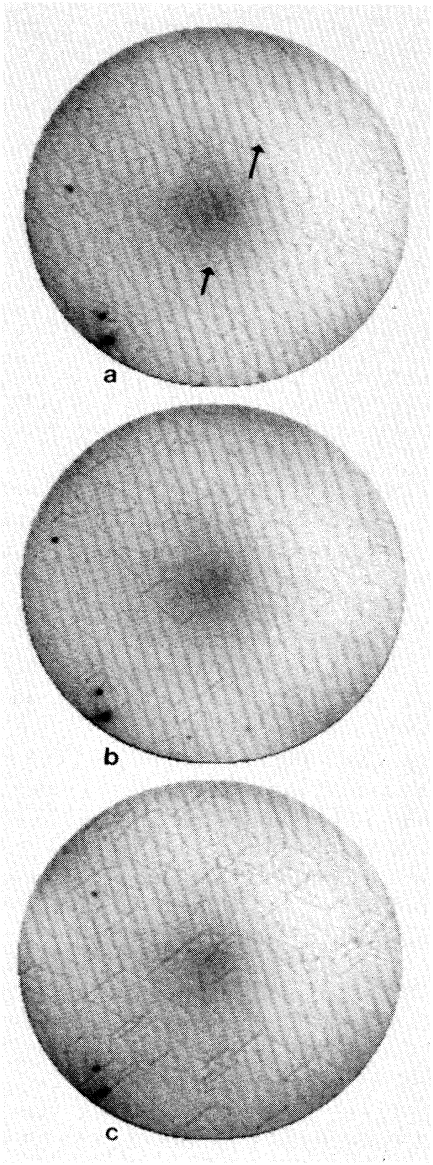

FIG. 1. Injection of misfit dislocations. Just above the critical thickness trigons (arrows) are nucleated near the center of the widest terraces (a). With increasing thickness [(b) and (c)] arms consisting of two partial dislocations (see Fig. 2) grow out from the corners of the trigons. The long diagonal lines are steps at the Si/CaF_2 interface, with partial dislocations character.

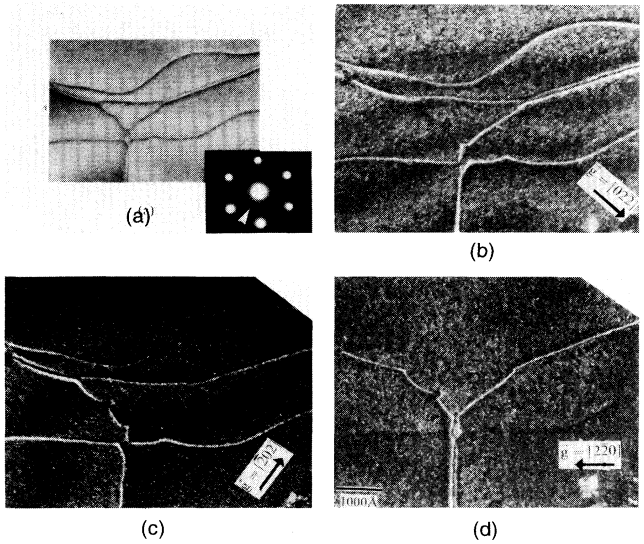

FIG. 2. (a) TEM bright field image of trigon plus dislocations arms, as seen in Fig. 1. Inset: transmission electron diffraction pattern with $1/3\langle 422 \rangle$ due to faulted region between partial dislocations in the arms. (b)–(d) Weak beam dark field images taken with indicated **g** diffraction vectors. Each of the dislocation lines (as well as the interface steps) are extinguished with the appropriate **g** vector.

(with LEEM) we have determined that the initial formation of the central triangle is accompanied by the appearance of a 2D island (a closed step loop) on the CaF_2 surface, showing that the dislocations associated with these triangles have a $1/3[111]$ component. We conclude that the central triangle is "squeezed" out of the film under the compressive strain in the film, reminiscent of the formation of stacking fault tetrahedra in strained films on Si(001). This occurs by the simultaneous nucleation of three $1/2\langle 110\rangle$ loops. Since these dislocations are inclined to the interface, their formation is accompanied by the appearance of the $1/3\langle 111\rangle$ surface step (i.e., a regular double-layer atomic step) on the surface, as observed with LEEM. The threading arms of the $1/2\langle 110\rangle$ half loops react with each other in the corners, preventing further glide. The corners are then natural sources for the full edge dislocations. The arms consist of pairs of partial dislocations, making up a full edge dislocation terminated by a threading dislocation. A schematic illustration of trigon plus arms is shown in Fig. 3. In Fig. 2(d) the two interface steps are also extinguished, as expected because of the partial dislocation character imparted by the B-type epitaxy. With the H_3 and T_4 adsorption sites related by a $1/6\langle 11\bar{2}\rangle$ translation vector, Ca occupies the H_3 site in the regions between the partial dislocations in the arms. This narrow region is ~200 Å wide, similar to the width of the two-dimensional structural modulation at the interface proposed by Huang *et al.* on the basis of x-ray scattering observations. Indeed, we believe that this structural modulation is a signature of the dislocation network observed directly here.

There has been some controversy over the adsorption site of Ca at the Si/CaF_2 interface [5,8,10,11]. Both

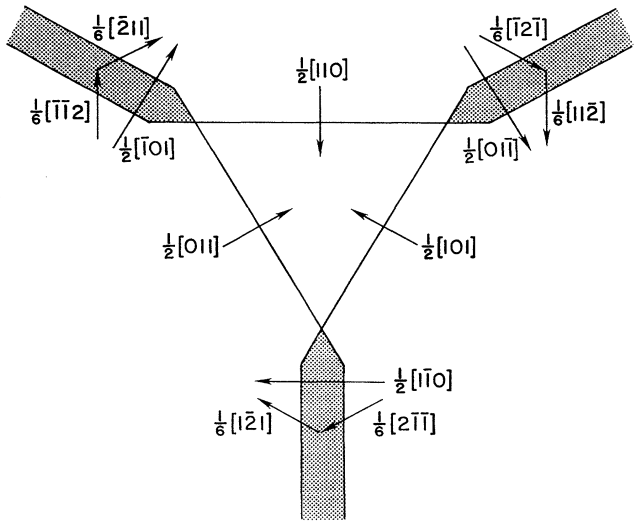

FIG. 3. Schematic illustration of trigon plus dislocation arms. Only the region between partial dislocations in the arms is faulted; the center triangular region is not.

x-ray studies, at 0.6 monolayer thickness [11] and at ~50 Å thickness [5], suggest the presence of interface Ca in both H_3 and T_4 sites, while ion scattering studies [8,10] of 1 monolayer films find only the T_4 site. Areas of H_3 and T_4 bonding geometry are necessarily separated by a partial dislocation which does *not* coincide with an interface step. Below the critical thickness the only partial dislocations observed are the interface steps, and the terraces display only one, unique interface bonding arrangement with Ca in the T_4 geometry [8,10,13]. Above the critical thickness partial dislocations are present in the terraces, and Ca occupies both T_4 and H_3 sites, a result of the nature of the dislocation network. The dislocation strain field extends to the surface of the CaF_2 film, analogous to dislocation strain fields at the $Si(111)/CoSi_2$ interface [14]. These long range strain fields were also observed in Ref. [5], as expected on the basis of elasticity theory [14].

The dislocation network in Figs. 1 and 2 is very sparse, as the critical thickness has just been exceeded. In Fig. 4(a) we show an image as the network is starting to densify in some regions, while in other regions only isolated dislocations are seen. One might expect the network to densify first in those regions where the film is somewhat thicker. Figure 4(b) shows an image of the CaF_2 surface taken a few seconds after Fig. 4(a). A regular array of steps is seen, as well as a few 2D islands on the larger terraces. However, the more densely dislocated areas in Fig. 4(a) do not correspond with thicker areas in Fig. 4(b). Instead, it appears that the nonuniformity of the dislocation network results from the statistical variations in dislocation nucleation, and the detailed local history of dislocation growth, highlighting the critical importance of the nucleation step. In Fig. 4(c) we show that the final network is dense and more uniform, as one would expect.

The misfit at 770 °C (2.4%) is much larger than at room temperature (0.6%), with CaF_2 having the larger lattice spacing. Thus, films grown at 770 °C are subject to thermal mismatch during cooling to room temperature. A previous room temperature atomic force microscope study of 1800 Å thick CaF_2 films grown on Si(111) at 750 °C concluded that the lattice mismatch during growth is, like the thermal mismatch, overcome by inclined glissile dislocations rather than by dislocations with Burgers vector parallel to the interface [3]. We have shown in the above that this is incorrect, and that lattice mismatch during growth at 770 °C is almost exclusively overcome by interface edge dislocations, which are apparently obscured by the high density of inclined glissile dislocations nucleated during cooling of the 1800 Å thick films. In our (much thinner) films we do not observe any sign of strain relief during cooling.

A dislocation structure similar to that described here was observed in the growth of Pd on Au(111) by Cherns and Stowell, although in that case the details of the initial dislocation nucleation were different (nucleation of dislocations on $\{11\bar{1}\}$ planes). The structure is also

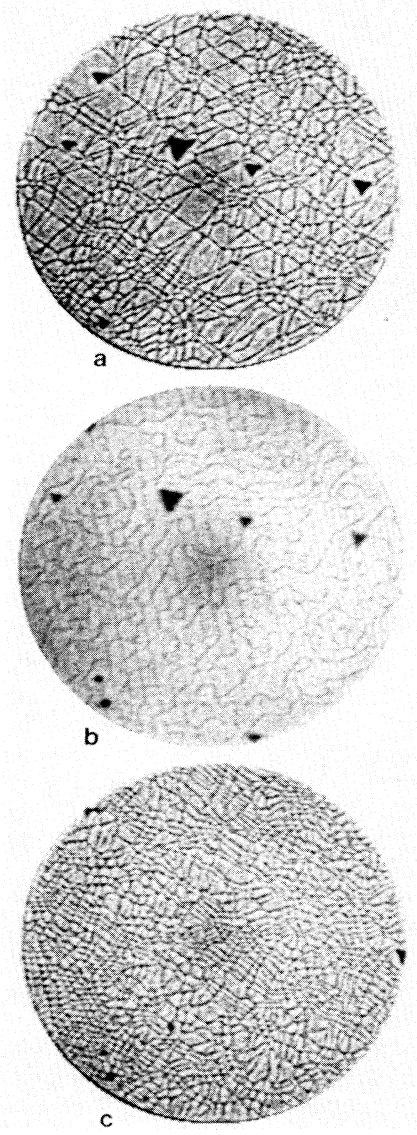

FIG. 4. (a) Dislocation network as it starts to densify. (b) Image of surface steps obtained one second after image (a). Regions of higher dislocation density do not correspond to regions of high surface step density (larger thickness), indicating that nonuniformity of dislocation density is not a result of thickness variations in the film, but of statistical variations in dislocation nucleation and growth. (c) Final dislocation network, showing uniform dislocation density.

remarkably similar to the structure of the adatom-induced reconstruction of the clean Pt(111) surface [15]. In the Pt case, however, the interior of the trigon contains a stacking fault, as well as the arms. Interestingly, this reconstruction is caused by a large compressive surface stress, analogous to the misfit strain in the (much thicker) CaF_2 films.

In conclusion, we have used *in situ* LEEM in combination with *ex situ* TEM to follow the relief of misfit strain as growth proceeds. During growth the misfit strain is relieved by a network of pure edge dislocations, with the Burgers vector in the interface plane. We obtain detailed information on the dislocation nucleation mechanism, and we identify the source of the edge dislocations. Interface Ca atoms shift from the Si T_4 to the Si H_3 adsorption site (and vice versa) at each interface partial misfit dislocation. We suggest that the two-dimensional structural modulation of the interface proposed in Ref. [5] corresponds to the two-dimensional strain-induced misfit dislocation network (and associated 3D strain fields) observed here in real space.

[1] J. W. Matthews and A. E. Blakeslee J. Cryst. Growth **27**, 118 (1974).
[2] D. Cherns and M. J. Stowell, Thin Solid Films **29**, 127 (1975).
[3] S. Blunier, H. Zogg, C. Maissen, A. N. Tiwari, R. M. Overney, H. Haefke, P. A. Buffat, and G. Kostorz, Phys. Rev. Lett. **68**, 3599 (1992).
[4] C. A. Lucas and D. Loretto, Appl. Phys. Lett. **60**, 2071 (1992); G. C. L. Wong, D. Loretto, E. Rotenberg, M. A. Olmstead, and C. A. Lucas, Phys. Rev. B **48**, 5716 (1993).
[5] K. G. Huang, J. Zegenhagen, Julia M. Phillips, and J. R. Patel, Phys. Rev. Lett. **72**, 2430 (1994).
[6] R. M. Tromp, A. W. Denier van der Gon, F. K. LeGoues, and M. C. Reuter, Phys. Rev. Lett. **71**, 3299 (1993).
[7] R. M. Tromp and M. C. Reuter, Ultramicroscopy **36**, 99 (1991).
[8] R. M. Tromp and M. C. Reuter, Phys. Rev. Lett. **61**, 1756 (1988).
[9] In *B*-type epitaxy the Burgers vector associated with an interface step depends on the sample miscut. Thus, depending on overlayer misfit and substrate miscut, interface steps may relieve or add strain to the overlayer. For an exactly lattice-matched overlayer interface steps always induce strain in the overlayer. For the samples studied here we have determined that interface steps relieve misfit strain..
[10] M. Katayama, B. V. King, E. Nomura, and M. Aono, Prog. Theor. Phys. Suppl. **106**, 315 (1991).
[11] J. Zegenhagen and J. R. Patel, Phys. Rev. B **41**, 5315 (1990).
[12] J. L. Batstone, J. M. Gibson, R. T. Tung, and A. F. J. Levi, Appl. Phys. Lett. **52**, 828 (1988).
[13] A possible explanation for the x-ray standing waves results of Ref. [10] is that below 1 monolayer the (1×1) T_4 structure coexists with lower coverage CaF_2 induced superstructures whose atomic arrangement is unknown. The experiments reflect an average of all structures present on the surface.
[14] R. Stalder, H. Sirringhaus, N. Onda, and H. von Känel, Ultramicroscopy **42–44**, 781 (1992).
[15] M. Bott, H. Hohage, T. Michely, and G. Comsa, Phys. Rev. Lett. **70**, 1489 (1993).

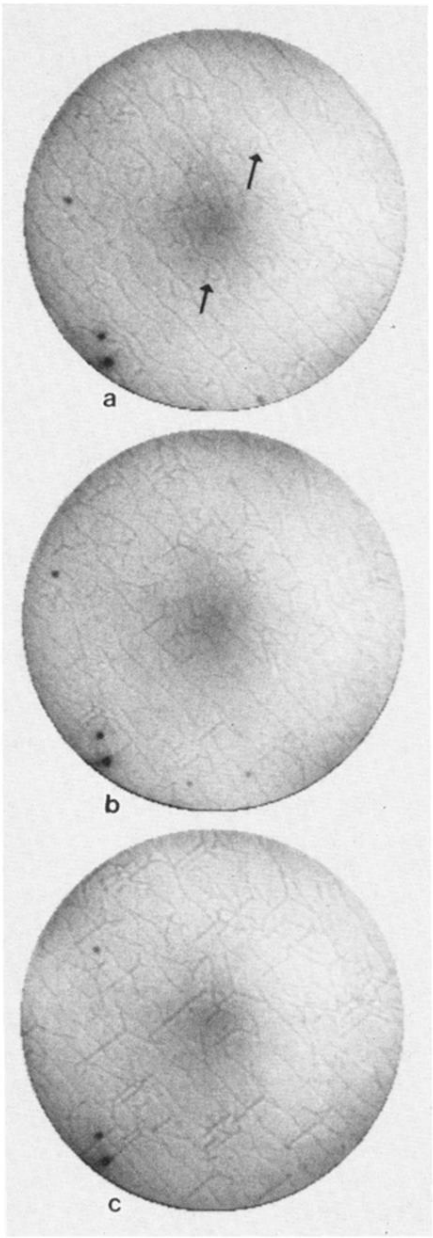

FIG. 1. Injection of misfit dislocations. Just above the critical thickness trigons (arrows) are nucleated near the center of the widest terraces (a). With increasing thickness [(b) and (c)] arms consisting of two partial dislocations (see Fig. 2) grow out from the corners of the trigons. The long diagonal lines are steps at the Si/CaF_2 interface, with partial dislocations character.

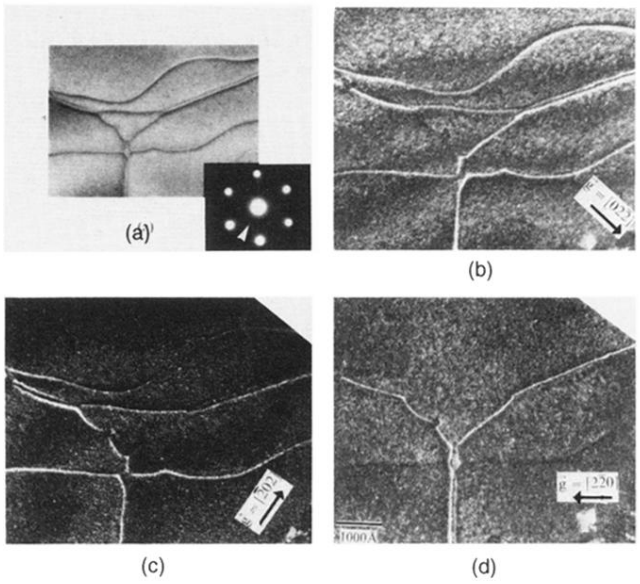

FIG. 2. (a) TEM bright field image of trigon plus dislocations arms, as seen in Fig. 1. Inset: transmission electron diffraction pattern with $1/3\langle 422\rangle$ due to faulted region between partial dislocations in the arms. (b)–(d) Weak beam dark field images taken with indicated **g** diffraction vectors. Each of the dislocation lines (as well as the interface steps) are extinguished with the appropriate **g** vector.

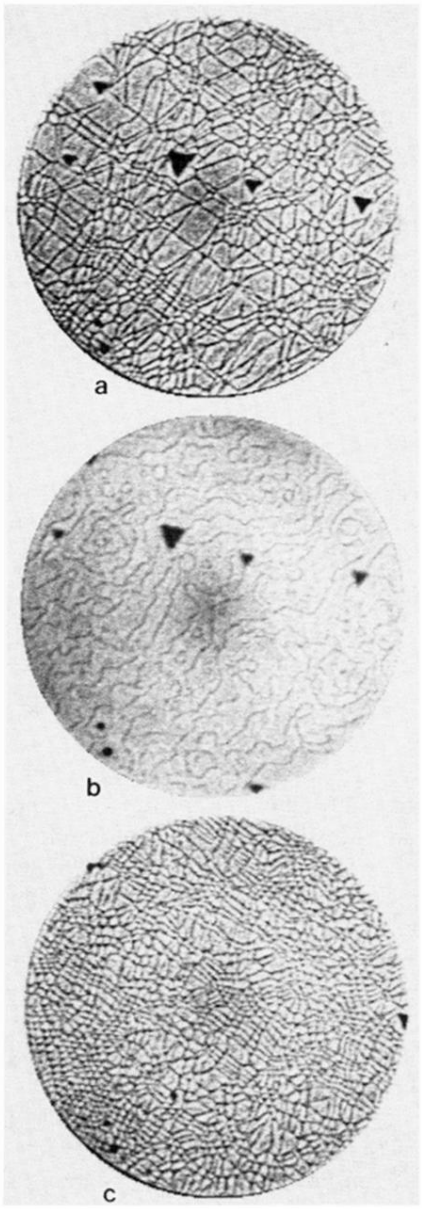

FIG. 4. (a) Dislocation network as it starts to densify. (b) Image of surface steps obtained one second after image (a). Regions of higher dislocation density do not correspond to regions of high surface step density (larger thickness), indicating that nonuniformity of dislocation density is not a result of thickness variations in the film, but of statistical variations in dislocation nucleation and growth. (c) Final dislocation network, showing uniform dislocation density.